Meteoritics 30, 387–398 (1995)

Nierite (Si_3N_4), a new mineral from ordinary and enstatite chondrites

MARTIN R. LEE[1*], SARA S. RUSSELL[2†], JOHN W. ARDEN[3] AND C. T. PILLINGER[2]

[1]Department of Physics, University of Essex, Colchester, Essex CO4 3SQ, U. K.
[2]Department of Earth Sciences, The Open University, Milton Keynes, MK7 6AA, U. K.
[3]Department of Earth Sciences, Oxford University, Oxford OX1 3PR, U. K.
*Present address: Department of Geology and Geophysics, University of Edinburgh, Edinburgh EH9 3JW, U. K.
†Present address: Department of Mineralogy, MRC-NHB 119, U. S. Museum of Natural History, Smithsonian Institution, Washington, D. C. 20560, USA

(Received 1994 December 1; accepted in revised form 1995 February 15)

Abstract–Nierite (Si_3N_4) is a new mineral that has been found in perchloric acid-resistant residues of three ordinary chondrites (Adrar 003 [LL3.2], Inman [L3.4] and Tieschitz [H3.6]) and one enstatite chondrite (Indarch [EH4]). This mineral occurs as very small (~2 × 0.4 μm) lath-shaped grains, which have been characterised by transmission electron microscopy. The d-spacings of nierite are, within errors, comparable to those of synthetic α-Si_3N_4, which has trigonal symmetry ($P31c$, a = 0.7758 nm, c = 0.5623 nm, V = 0.2931 nm^3, Z = 4). Energy-dispersive x-ray analyses confirm that nierite is a Si- and N-rich mineral. A few nierite crystals in the Indarch, Inman and Tieschitz residues are intergrown with whiskers of another nitride. Only two crystals of this additional nitride were found that were of sufficient size to give electron diffraction patterns uncontaminated by nierite reflections. The d-spacings of this second nitride are comparable to those of β-Si_3N_4, the hexagonal polymorph of synthetic Si_3N_4.

The majority of nierite crystals in Indarch are interpreted to have formed by exsolution of Si and N from kamacite, perryite and schreibersite during parent-body metamorphism. Some grains have evidence for two discrete episodes of nierite crystallization. The origin of nierite in Adrar 003, Inman and Tieschitz is not known, but formation during exsolution is again possible. The petrographic relationships between nierite and β-Si_3N_4 in Indarch, Inman and Tieschitz suggests that the β-Si_3N_4 whiskers predated nierite and acted as a seed on which nierite crystals later nucleated. The nierite/β-Si_3N_4 ratio in ordinary chondrites is controlled by their metamorphic grade and possibly also their oxidation state.

INTRODUCTION

It is now well established that perchloric acid-resistant residues of primitive meteorites contain components whose anomalous isotopic composition cannot readily be explained by mass fractionation processes in the solar nebula. The character of these isotopic anomalies indicates a presolar origin. Mineralogical analysis of these residues by scanning and transmission electron microscopy has shown that the carrier phases of the isotopic anomalies include nm-sized diamonds (nanodiamonds) (Lewis *et al.*, 1987), μm and sub-μm-sized silicon carbide (SiC) grains (Bernatowitcz *et al.*, 1987), graphite spheres (Amari *et al.*, 1990), titanium carbide (TiC) inclusions within graphite and SiC (Bernatowicz *et al.*, 1991) and corundum (Huss *et al.*, 1992; Nittler *et al.*, 1993). However, there are potentially many more presolar minerals to be found, and amongst the most promising candidates are nitrides.

A number of N-bearing minerals from meteoritics have been previously described. They include sinoite (Si_2N_2O) (Andersen *et al.*, 1964), which occurs in enstatite chondrites, and osbornite (TiN), which has been described from the Bustee aubrite by Bannister (1941). It is also inferred to occur in a number of E6 chondrites (Grady *et al.*, 1986). Recent interest, however, has centred on silicon nitride (Si_3N_4) that has been tentatively identified from two enstatite chondrites, Qingzhen (EH3) (Alexander *et al.*, 1991, 1994; Huss *et al.*, 1995) and Indarch (EH4) (Stone *et al.*, 1991a,b; Alexander *et al.*, 1994) and one ordinary chondrite, Tieschitz (H3.6) (Alexander, 1993). Hoppe *et al.* (1994) have described a Si- and N-rich mineral from Murchison (CM2) but could not determine whether it was Si_3N_4 or sinoite. Most of the Si_3N_4 in enstatite chondrites has an isotopic composition within error of terrestrial values (Alexander *et al.*, 1994), but ion microprobe analysis of grains from Murchison, Tieschitz and Qingzhen has shown that they are isotopically anomalous and possibly presolar (Hoppe *et al.*, 1994; Alexander, 1993; Huss *et al.*, 1995). Isotopic analysis of perchloric acid-resistant residues of Si_3N_4-bearing meteorites by stepped combustion has confirmed that a significant difference in overall N-isotopic composition exists between the Si_3N_4 population in ordinary and in enstatite chondrites (Lee *et al.*, 1992; Russell *et al.*, 1995).

It is the purpose of this paper, which is a companion to the paper by Russell *et al.* (1995), to describe the crystallography and petrography of Si_3N_4 from perchloric acid-resistant residues of three ordinary chondrites (Adrar 003 [LL3.2], Inman [L3.4] and Tieschitz [H3.6]) and one enstatite chondrite (Indarch [EH4]). In particular, we have attempted to ascertain whether any mineralogical differences exist between Si_3N_4 in the ordinary and enstatite chondrites, which can be related to distinct contrasts in their isotopic composition described by Lee *et al.* (1992) and Russell *et al.* (1995). During the course of this work, it became apparent that the majority of Si_3N_4 crystals in the meteorite residues are chemically and crystallographically comparable to the trigonal polymorph of synthetic Si_3N_4, called α-Si_3N_4. This is the first confirmed occurrence of trigonal Si_3N_4 in nature. This new mineral and its name, nierite, has recently been approved by the Commission on New Minerals and New Mineral Names of the International Mineralogical Association. A 3.05-mm diameter perforated C film that contains a nierite-bearing perchloric acid-resistant residue of Indarch has been placed with the British Museum (Natural History). We have named this mineral nierite in

honour of the late A. O. C. Nier (1912–1994). He was responsible for the now accepted measurement of the atmospheric N-isotopic composition (Nier, 1950) and was one of the founding fathers of mass spectrometry in general and stable isotope mass spectrometry in particular.

EXPERIMENTAL

All of the samples investigated in this study were perchloric acid-resistant residues. To produce these residues, samples of the meteorites were etched in HF and HCl, then broken into small pieces and treated with 9M HF/1M HCl, CS_2, 0.4M $Cr_2O_7^{2-}$ and $HClO_4$. The residues were then heated under an infrared lamp for a few hours, washed in water, then acetone and finally dried. No attempt was made to conduct further chemical or physical mineral separation. The weight of the perchloric acid-resistant residue associated with total weight of the sample was 165 ppm for Adrar 003, 42 ppm for Indarch, 93 ppm for Inman and 127 ppm for Tieschitz. For a discussion regarding the possibility that samples were contaminated with debris from rock, saws, *etc.*, the reader is referred to Russell *et al.* (1992b). The samples studied here were treated in a similar manner to the Abee specimen. Indarch and Adrar 003 had between 5 and 7% of their mass etched away and discarded from cut surfaces prior to breaking into small pieces. Inman was etched until the surface appeared rough. Only Tieschitz was not so treated because the sample had no cut surfaces, and it was described "as from an interior chip."

Samples of the perchloric acid-resistant residues were prepared for study by transmission electron microscopy (TEM) as follows. Firstly, a few drops of isopropanol was mixed with the residues in a glass phial under clean room conditions and then agitated by ultrasound until the residue was in suspension. A couple of drops of the liquid were then pipetted on to perforated C films supported by a Cu grid, comprised of several hundred grid squares 60 μm^2 in size, and briefly dried. The residue is rarely uniformly distributed over the C film and tends to be denser in some areas than in others. The abundance of Si_3N_4 grains per unit area of the C film was calculated during this study but owing to the aforementioned contrasts in sample density over the surface of the film, these data are only semiquantitative. These residues were studied using a JEOL 200CX transmission electron microscope (TEM) operated at 200kV for imaging, electron diffraction and qualitative x-ray analysis. Most mineral grains were sufficiently thin to transmit electrons, and so it was not necessary to process them further by, for example, ion-beam thinning. Crystals of Si_3N_4 were located by systematically traversing the C film and analysing all likely grains using a Link Systems ultra-thin window energy-dispersive x-ray detector, which can qualitatively analyse for elements of atomic number >5. Additional images and electron diffraction data was acquired using a Philips CM12 TEM operated at 120kV and equipped with a Gatan image intensifier to aid high-resolution imaging.

The C films were mounted in an eucentric double-tilt goniometer specimen holder for acquisition of selected area electron diffraction (SAED) patterns. In many SAED patterns of Si_3N_4 single crystals, continuous smooth diffraction rings from nanodiamonds were superimposed on the spot patterns. This is caused by encrustation of the mineral grains by nanodiamonds, which are abundant in these meteorite residues (Russell *et al.*, 1991, 1992a), during sample preparation. The nanodiamond diffraction rings, however, provided an excellent internal standard for calibrating the SAED patterns of Si_3N_4. The innermost {111} diffraction ring of nanodiamonds was assumed to have a d-spacing of 0.206 nm.

Quantitative chemical analyses of Si_3N_4 grains were obtained using a Fisons HB601UX scanning transmission electron microscope (STEM) equipped with an Oxford Instruments windowless energy-dispersive x-ray detector and a Gatan parallel EELS spectrometer. This instrument was operated at 100 kV, with an analytical probe size of 1 nm and a 0.5 nA probe current. Acquired spectra were quantified using the thin film technique of Cliff and Lorimer (1975). The K-factors for N were calculated from x-ray spectra of synthetic Si_3N_4. Potential Si_3N_4-bearing crystals of kamacite, perryite, schreibersite and troilite in a polished block of Qingzhen and a polished thin section of Indarch were analysed using a Cameca Camebax wavelength-dispersive electron microprobe. An accelerating voltage of 20 kV and beam current of 10 nA were used.

MINERALOGY OF THE PERCHLORIC ACID-RESISTANT RESIDUES

Non-Nitride Phases

All of the four perchloric acid-resistant residues contained μm- to sub-μm sized grains of spinel, chromite, hibonite and rutile. A Na-Cr silicate, possibly ureyite, was found in Indarch and Inman and was very common in the Tieschitz residue. In addition, nanodiamonds were abundant in all of the residues. Silicon carbide was found in three of the residues (Indarch, Inman and Tieschitz) and is briefly described later.

Nitrides

From indexed SAED patterns and TEM images, two crystallographically and morphologically distinct Si- and N-rich phases have been identified from the four acid-resistant residues studied by TEM. The most abundant phase, which occurs in all four residues, forms lath-shaped crystals ~2.0 × 0.4 μm whose d-spacings in SAED patterns agree very well with those of the trigonal polymorph of synthetic Si_3N_4, called α-Si_3N_4. Only two crystals of the other nitride were found (one in Inman and one in Tieschitz) that were sufficiently large to produce good SAED patterns. The d-spacings of this phase, measured from SAED patterns and high-resolution TEM images, are consistent with those of the hexagonal polymorph of synthetic Si_3N_4, or β-Si_3N_4.

A sufficient number of crystals of the phase comparable to synthetic α-Si_3N_4 were available for its crystallographic characteristics and chemical composition to be determined with confidence, and we have called this new mineral nierite. Far fewer crystals of the phase whose d-spacings are consistent with synthetic β-Si_3N_4 were found, and a comprehensive study of its crystallographic characteristics and chemical composition was not possible. This phase is, therefore, referred to throughout as β-Si_3N_4. In cases where meteoritic Si_3N_4 has been identified but its polymorph is not known, it is referred to as Si_3N_4.

Properties of Synthetic Silicon Nitride

Crystallography–The unit-cell parameters of synthetic α-Si_3N_4 have been measured many times, but these values are variable, the degree of variation often being beyond experimental errors (Table 1). These contrasts are probably due to differences in manufacturing conditions, changing the nature and concentration of impurities in the structure; the main contaminant is probably O (Wild *et al.*, 1972). Here we have used the crystallographic properties for α- and β-Si_3N_4 calculated by Forgeng and Decker (1958) (Table 2), because these authors have published unit-cell parameters and complete x-ray powder data for both polymorphs;

TABLE 1. Selection of determinations of the unit-cell parameters of synthetic α-Si_3N_4.

Unit-cell parameters a (nm)	c (nm)	Reference
0.7748 (1)	0.5617 (1)	Hardie and Jack, 1957
0.7758 (5)	0.5623 (5)	Forgeng and Decker, 1958
0.7753 (4)	0.5618 (4)	Ruddleston and Popper, 1958
0.7765 (1)	0.5622 (1)	Marchand *et al.*, 1969
0.77520 (7)	0.56198 (5)	Wild *et al.*, 1972*
0.77533 (8)	0.56167 (6)	Wild *et al.*, 1972**
0.7766 (10)	0.5615 (8)	Kohatsu and McCauley, 1974
0.7818 (3)	0.5591 (4)	Kato *et al.*, 1975
0.77491 (5) to 0.77572 (5)	0.56164 (5) to 0.56221 (5)	Jack, 1983*** "

Number in parenthesis is the standard deviation of the last significant figure.
* = determined from α-Si_3N_4 wool,
** = determined from α-Si_3N_4 needles.
*** Range of values calculated from 26 different specimens manufactured using 3 different techniques.

TABLE 2. Basic properties of synthetic Si_3N_4 (from Forgeng and Decker, 1958).

	α-Si_3N_4	β-Si_3N_4
Crystal system:	Trigonal	Hexagonal
Space group:	$P31c$	$P6_3/m$
Unit-cell parameters:	a = 0.7758 (5) nm	a = 0.7603 (5) nm
	c = 0.5623 (5) nm	c = 0.2909 (3) nm
	V = 0.2931 nm^3	V = 0.1456 nm^3
	Z = 4	Z = 2

Number in parenthesis is the standard deviation of the last significant figure.

TABLE 3. The five strongest lines in x-ray powder patterns of both of the polymorphs of synthetic Si_3N_4.

Synthetic α-Si_3N_4			Synthetic β-Si_3N_4		
I	$d_{meas.}$ (nm)	hk.l	I	$d_{meas.}$ (nm)	hk.l
100	0.2547	21.0	100	0.1.41	32.1
85	0.2893	20.1	70	0.2668	10.1
75	0.1351	32.2	70	0.3492	21.0
75	0.2599	10.2	60	0.331	20.0
70	0.1486	32.1	60	0.1228	41.1

Data from Forgeng and Decker (1958).

their data for α-Si_3N_4 is also tabulated in J.C.P.D.S. card no. 9-250. The five strongest lines in x-ray powder patterns of both polymorphs of synthetic Si_3N_4, again from Forgeng and Decker (1958), are listed in Table 3.

Chemistry–The unit-cell formula of α-Si_3N_4 is $Si_{12}N_{16}$. There are four sites for N atoms and two for Si atoms in the unit-cell. As already stated, variability in unit-cell parameters (Table 1) has led to a proposal by Wild *et al.* (1972) that α-Si_3N_4 can contain significant concentrations of O and should, more correctly, be called an oxynitride. Wild *et al.* (1972) suggested that O partially replaces N in the N(1) site of synthetic α-Si_3N_4 and is accompanied by vacancies in the N(4) site and Si sites, giving a composition $Si_{11.5}N_{15}O_{0.5}$, corresponding to 0.9–1.5 wt% O. Furthermore, Wild *et al.* (1972) postulated that the presence of O in some N sites was essential for the structural stability of synthetic α-Si_3N_4. Detailed chemical analysis of synthetic α-Si_3N_4 using neutron activation analysis, in addition to further x-ray structural refinements, has shown however that the compound typically contains <0.3 wt% O and does not require O for structural stability (Priest *et al.*, 1973; Kato *et al.*, 1975; Jack, 1983).

Other Properties of Synthetic α-Silicon Nitride–The physical and optical properties of synthetic α-Si_3N_4 have received little attention. The calculated density of stoichiometric synthetic α-Si_3N_4 is 3.184 g/cm^3 (Hardie and Jack, 1957). This is close to the measured density of single crystals, for example Niihara and Hirai (1979) obtained values of 3.17–3.18 g/cm^3, which is greater than the range 3.167–3.171 g/cm^3 recorded by Wild *et al.* (1972). Again, the difference is attributed by the latter authors to O substitution and resultant vacancies in the structure. Synthetic α-Si_3N_4 has a hardness of nine on Mohs' scale, and Niihara and Hirai (1979) have demonstrated that the Knoop hardness of single α-Si_3N_4 crystals is anisotropic, ranging from 2600–3500 kg/mm^{-2} (100g load, 0.3 mm/s^{-1} loading rate, 10 s loading time, measured at room temperature).

Pure synthetic α-Si_3N_4 is transparent and colourless, because its optical absorption edge is ~310 nm. But with increasing O content, single crystals may become brown to brownish-red (Niihara and Hirai, 1979). Preliminary optical data for synthetic Si_3N_4 were reported by Forgeng and Decker (1958), and a more complete study was conducted by Clancy (1974). He found that α-Si_3N_4 is uniaxial (–) (ω = 2.03, ϵ = 2.02), whereas β-Si_3N_4 is uniaxial (+) (ω = 2.02, ϵ = 2.04). Taylor (1973) measured the reflectivity of α-Si_3N_4 and β-Si_3N_4, which is 12.2% for both polymorphs.

TABLE 4. Comparison between the measured and calculated d-spacings of synthetic α-Si_3N_4 and nierite.

Synthetic α-Si_3N_4			Nierite				
			(1)		(2)		(3)
hk.l	$d_{meas.}$(nm)	$d_{calc.}$ (nm)	$d_{meas.}$(nm) mean	n	$d_{meas.}$(nm) mean	n	$d_{calc.}$ (nm)
10.0	0.669	0.6719	0.670 (2)	17	0.673 (6)	14	0.670
00.1	-------	0.5623	0.561 (2)	16	0.561 (6)	14	0.561
10.1	0.432	0.4312	0.431 (2)	32	0.430 (5)	25	0.430
11.0	0.388	0.3879	0.388 (1)	7	0.391 (0)	3	0.387
20.0	0.337	0.3359	0.335 (1)	17	0.337 (3)	14	0.335
11.1	--------	0.3193	0.318 (1)	6	0.318 (1)	2	0.319
20.1	0.2893	0.2884	0.287 (1)	28	0.288 (3)	22	0.228
00.2	0.2823	0.2812	0.281 (1)	17	0.280 (3)	14	0.281
10.2	0.2599	0.2594	0.259 (1)	28	0.259 (3)	23	0.259
21.0	0.2547	0.2539	0.254 (1)	8	0.254 (3)	6	0.253
21.1	0.2320	0.2314	0.230 (1)	8	0.231 (2)	6	0.231
11.2	0.2283	0.2276	0.228 (1)	3	0.227 (0)	3	0.227
30.0	0.2244	0.2240	0.223 (1)	17	0.224 (2)	14	0.223
20.2	0.2158	0.2156	0.215 (1)	32	0.215 (3)	25	0.215
30.1	0.2083	0.2081	0.208 (0)	2	0.211 (0)	2	0.208
22.0	0.1937	0.1940	0.194 (1)	7	0.196 (0)	3	0.194
21.2	0.1884	0.1885	0.188 (0)	2	0.188 (0)	2	0.188
00.3	---------	0.1874	0.187 (1)	16	0.187 (2)	14	0.187

Measured d-spacings for synthetic α-Si_3N_4 calculated from x-ray powder data by Forgeng and Decker (1958).

------ = reflection not present. The calculated d-spacings for synthetic α-Si_3N_4 were determined here using cell parameters of a = 0.7758 (5) nm, c = 0.5623 (5) nm. The d-spacing data for nierite were calculated from indexed SAED patterns of a number of different zone axes. Data in column (1) was obtained from SAED patterns whose camera factor had been quantified using the {111} diffraction ring of nanodiamonds. Data in column (2) was determined using an average value of the camera factor. Numbers in parenthesis are the standard deviation of the last significant figure. n denotes the number of different reflections that were measured. Data in column (3) are d-spacings for nierite calculated using unit cell parameters of a = 0.774 (2) nm, c = 0.561 (2) nm.

Properties of Nierite

Difficulties in the Study–The very small size of all of the nierite crystals encountered during this study (~2 × 0.4 μm) has put severe limitations on the degree to which the crystals could be characterised. No measurements of physical or optical properties could be made, and it was not possible to obtain sufficient residue for x-ray structure determinations without destroying enormous quantities of precious meteorites. The abundances of Si_3N_4 in the bulk meteorites are as follows: Adrar 003 = 148 ppb; Indarch = 706 ppb; Inman = 27 ppb; Tieschitz = 12 ppb (Russell *et al.*, 1995).

The identification of nierite as a new mineral has been on the basis of demonstrating, by electron diffraction and energy-dispersive x-ray analysis in the TEM, that nierite is crystallographically and chemically comparable to syn-

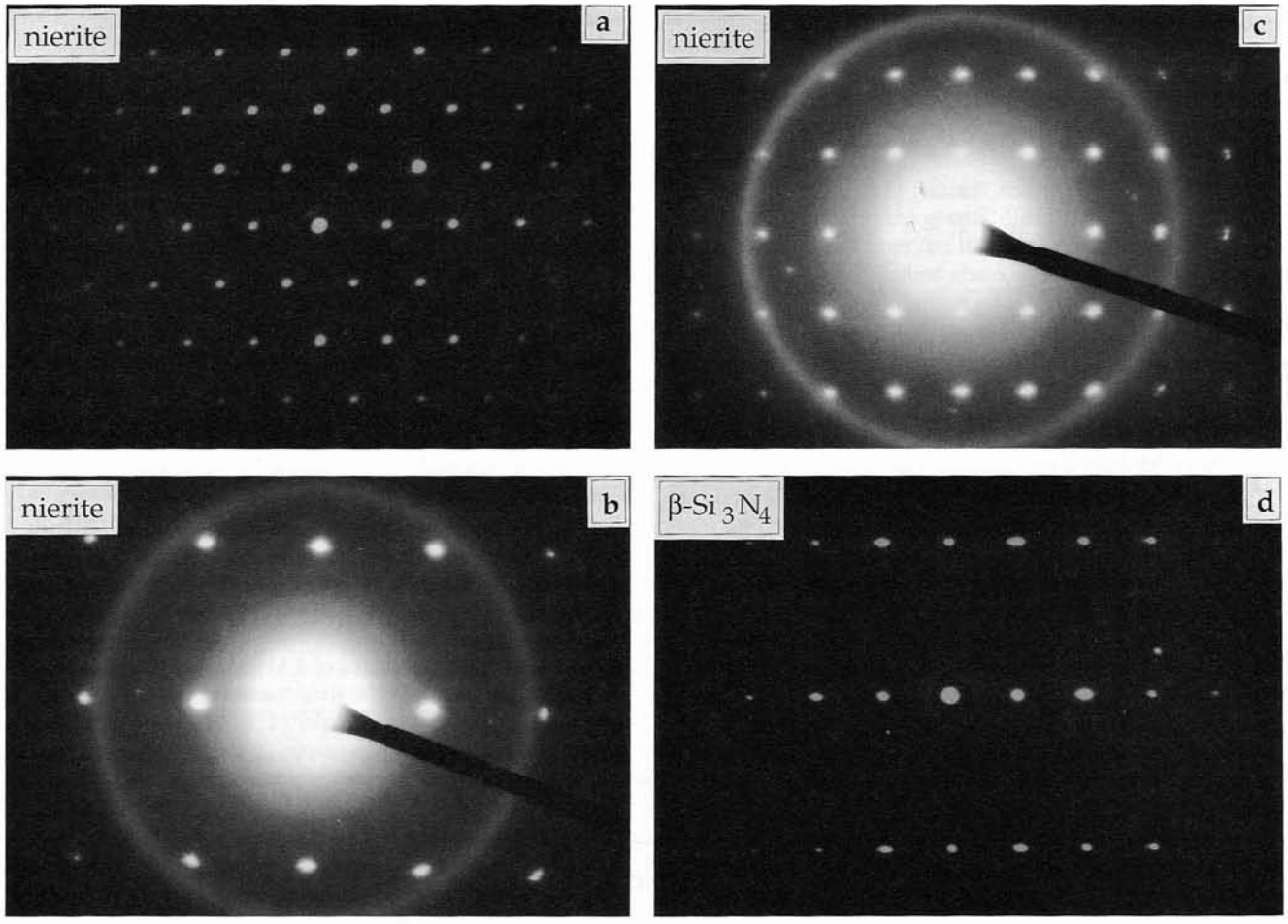

FIG. 1. The SAED patterns of meteoritic Si_3N_4. (a) <0001> pattern of nierite from Indarch; (b) $< 10\bar{1}0 >$ pattern of nierite from Adrar 003; (c) $< 11\bar{2}0 >$ pattern of nierite from Adrar 003; (d) $< 11\bar{2}0 >$ pattern of β-Si_3N_4 from Tieschitz. The SAED patterns in (b) and (c) also contain the {111} nanodiamond diffraction ring.

thetic α-Si_3N_4, whose crystallographic, physical and optical properties have been described above.

Crystallography–Tens of SAED patterns from a variety of zone axes were obtained from nierite grains in all four of the acid-resistant residues (Fig. 1). Many of these SAED patterns contained the {111} diffraction ring from nanodiamonds superimposed on the regular array of spots originating from nierite (Figs. 1b,c). In these cases, the camera factor for the TEM could be calibrated and d-spacings accurately found. The d-spacings calculated from these calibrated SAED patterns (Table 4, column 1), together with measured interplanar angles, are in close agreement with those of synthetic α-Si_3N_4. Other SAED patterns of nierite were available in which the {111} nanodiamond diffraction ring was absent or too faint to measure sufficiently accurately for calibration purposes (Fig. 1a); in these cases, an average value of the camera factor of the microscope was employed. Inevitably, d-spacings estimated from the standardless SAED patterns (Table 4, column 2) are less accurate than those from the internally-calibrated patterns.

The unit-cell parameters of nierite calculated from measured d-spacings (Table 4, column 1) are: a = 0.774 ± 0.002 nm, c = 0.561 ± 0.002 nm. These unit-cell parameters have been used to calculate ideal d-spacings for the new mineral (Table 4, column 3). The density of nierite calculated from the crystallographic and chemical data reported here is 3.11 g/cm^3 (J. Mandarino, pers. comm., 1994).

Chemical Composition–The nierite grains found in this study were too small for reliable chemical analysis by electron microprobe, and so the chemical compositions of crystals from Indarch were established by using an analytical STEM. In addition to peaks from Si and N, x-ray spectra from the nierite crystals also contained C and O peaks (Fig. 2). Element maps of a single crystal show that the C and O is not uniformly distributed but is concentrated in discrete "clumps," which is consistent with an origin mainly from contamination. The C undoubtedly comes from nanodiamonds, which TEM images and SAED patterns show encrusting the surfaces of nierite grains. Stepped pyrolysis of nanodiamond samples shows that up to ~10% of their mass can be released as labile CO_2 at temperatures <600 °C (Verchovsky *et al.*, 1993). This component is interpreted to be related to the "carboxyl functional groups" that convey acidic properties to the nanodiamonds (Lewis *et al.*, 1989). It is unknown whether these properties of the diamond are artifacts of the isolation procedure. However, it is highly likely that the O seen here is associated with nanodiamond, and qualitatively the C/O ratio seen in Fig. 2 is of the right order.

As previously stated, synthetic α-Si_3N_4 may itself contain minor concentrations (<0.3 wt%) of O, which probably substitutes for N in the lattice. However, given the known contamination by nanodiamond-derived O, it was not possible to place any limits on the degree of O substitution in the lattice of nierite crystals.

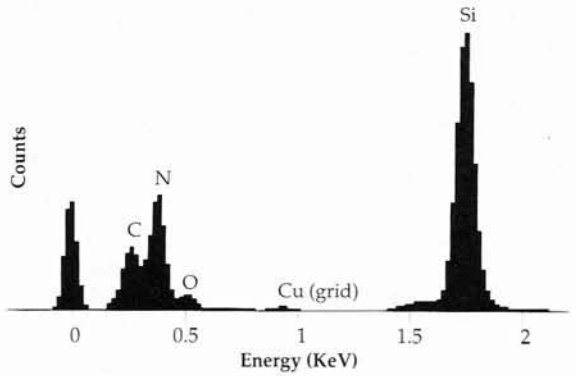

FIG. 2. Energy-dispersive x-ray spectrum obtained from a nierite grain in the Indarch residue. The main peaks are from N and Si, but there is also a substantial contribution from C and O. The small Cu $L_{\alpha 1}$ peak is produced by the Cu grid, which supports the perforated C film.

For quantitative x-ray analysis, C and O peaks were stripped from the spectra of nierite. The concentration of Si and N in different crystals and between different parts of individual crystals is variable, and qualitatively the N concentration is proportional to the size of the C peak in the untreated x-ray spectra (Table 5). This is interpreted to indicate that the nanodiamonds have significant concentrations of N. Although we did not quantify the concentration of N in nanodiamonds, our qualitative observations are in keeping with the stepped-combustion results of Russell *et al.* (1991), which suggests that Indarch nanodiamonds have ~0.5 wt% N. Quantified x-ray spectra of nierite that have the smallest C peaks are closest in composition to stoichiometric Si_3N_4 (60 wt% Si, 40 wt% N) (Table 5).

Electron Petrography of Nierite and β-Silicon Nitride in Meteorite Residues

Adrar 003–This residue was not available in sufficient quantities to provide a good TEM specimen. However, one ragged grain of nierite was found. The grain is a sub-euhedral lath, 1400 nm long × 200 nm wide (Fig. 3a). The long axis of the lath is oriented parallel to c*.

Indarch–Nierite is very abundant in the Indarch residue with between 10 and 30 grains occurring on every 60 μm^2 of C film.

TABLE 5. Chemical composition of nierite from Indarch.

N (wt%)	Si (wt%)	Qualitative C/N ratio
45	55	3
42	58	2.5
47	53	1.25
46	54	1.25
44	56	0.6
40	60	0.5
40	60	0.25
38	62	0.25

Si and N determinations by quantitative STEM from three different nierite grains. Data accurate to ±2 wt%.

All grains in the residue are separate such that no indication of any former petrographic relationships remain. Most grains have a lath or acicular morphology and are 970–4925 nm long (mean = 2060 nm) (n = 16) × 110–720 nm wide (mean = 320 nm) and have length/width ratios ranging from 3.6–22.8 (mean = 7.1) (Fig. 3b). The majority of the grains are transparent to 200 kV electrons and so are < ~100–200 nm in thickness. An insufficient number of crystals could be oriented with their <0001> zone axes parallel to the electron beam for their cross-sectional morphology to be investigated.

Nearly all nierite grains are single crystals with their long axes oriented parallel to c* (Fig. 3b). The majority of crystals are euhedral, and their faces lie parallel to lattice planes (Fig. 3b). However, some of the smaller crystals are clearly fragments of larger grains. The timing of grain breakage relative to sample preparation is not known.

Five nierite laths were found that contain a central parallel-sided band, <50.0 nm in width, which gives them a segmented appearance (Figs 4a, b). Qualitative x-ray analysis showed no discernible compositional difference between pure nierite and regions of the crystal that contained the bands. The bands were too small to obtain good SAED patterns from, but faint extra reflections were seen in some $<11\bar{2}0>$ diffraction patterns with d-spacings of ~0.29 and ~0.26 nm. One set of lattice fringes, spacing ~0.66 nm, could be discerned on high-resolution images of the

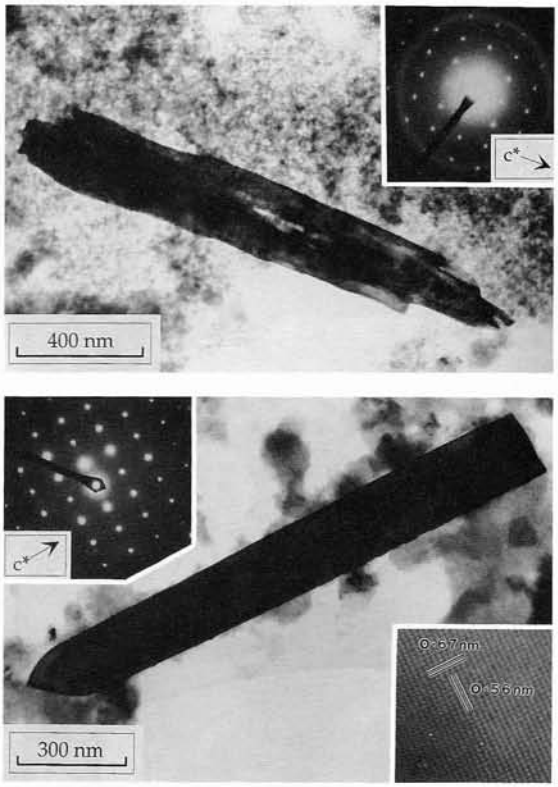

FIG. 3. Nierite crystals from Adrar 003 and Indarch. (a, upper) Bright-field TEM image and corresponding $<11\bar{2}0>$ SAED pattern (inset) of the only nierite crystal found in the residue of Adrar 003. (b, lower) Bright-field TEM image with corresponding $<11\bar{2}0>$ SAED pattern (inset, top left) and high-resolution image (inset, bottom right) of a typical nierite crystal from the Indarch residue. This crystal is sufficiently thin for small clumps of nanodiamonds that lie beneath it to be seen. The curved structure in the bottom of the image is a hole in the C film.

bands, parallel to the $(01\bar{1}0)$ lattice fringes of host nierite. The d-spacings of ~0.66, ~0.29 and ~0.26 nm from the bands are consistent with the spacing of the $(01\bar{1}0)$, (0001) and $(01\bar{1}1)$ planes in β-Si_3N_4 (0.663, 0.291 and 0.267 nm, respectively) (Table 6). In these five bimineralic grains, nierite and β-Si_3N_4 have an epitaxial relationship, whereby $<11\bar{2}0>_{\text{nierite}} || <11\bar{2}0>_{\beta\text{-}Si_3N_4}$.

In two cases, tiny rectangular pores, ~4 nm × 2.5 nm, were found within the β-Si_3N_4 bands. These pores have the shape of negative crystals and are bounded by the $(01\bar{1}0)$ planes of β-Si_3N_4 and the (0001)-parallel interface between nierite and β-Si_3N_4. In no cases were such pores found within monocrystalline nierite grains. They must, therefore, have formed selectively within the β-Si_3N_4 bands and may reflect a difference in the resistance of β-Si_3N_4 and nierite to the residue preparation.

In addition to the β-Si_3N_4 bands, some nierite crystals also contain narrow, parallel-sided defects, which are oriented with their long axes parallel to (0001) lattice fringes when looking down $<11\bar{2}0>$ (Fig. 5). These defects are ≤2.8 nm in width (*i.e.*, ≤5 (0001) lattice fringe repeats) and are comparable in size and crystallographic orientation to (0001) planar defects described from synthetic α-Si_3N_4 whiskers by Sasaki *et al.* (1985). From high-resolution TEM images, these authors calculated the displacement vector, $\vec{R}$, of the planar defects to be $\frac{1}{2}a<10\bar{1}0>$. Planar defects are most numerous where the (0001)-parallel end of a nierite grain is epitaxially overgrown by another nierite crystal (Fig. 5). These overgrowths have thus crystallized in a manner that appears to have encouraged the formation of planar defects.

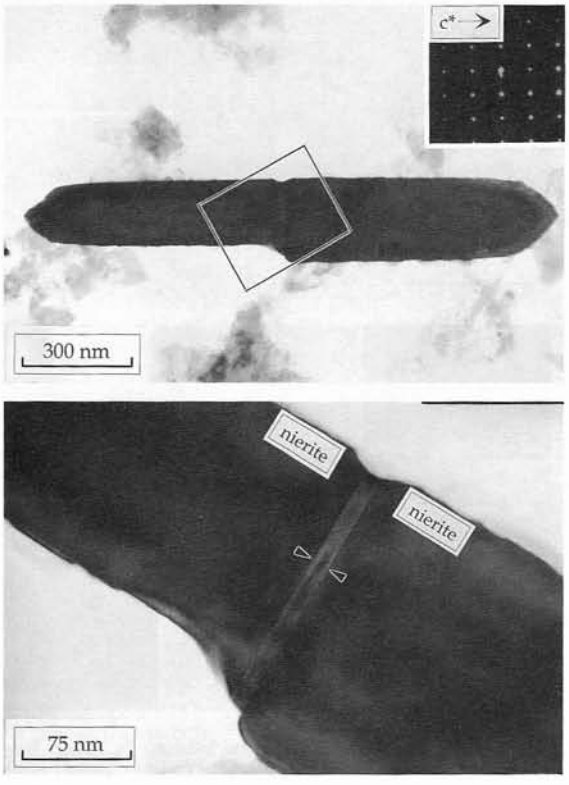

FIG. 4. A bimineralic Si_3N_4 grain from the Indarch residue. (a, upper) Bright-field TEM image and corresponding $<11\bar{2}0>$ SAED pattern of the crystal (inset). (b, lower) Higher magnification image of the middle of the crystal (boxed area in 4a) showing a narrow band of β-Si_3N_4 (delineated by arrows).

Small (<200 nm) SiC grains (Wright, 1992) are ubiquitous in the Indarch residue. The d-spacings of these SiC grains are consistent with those of the cubic polytype of SiC.

TABLE 6. Comparison between the d-spacings of synthetic and meteoritic β-Si_3N_4.

	Synthetic β-Si_3N_4		**Meteoritic β-Si_3N_4**	
hk.l	$d_{meas.}$(nm)	$d_{calc.}$ (nm)	(1) d (nm)	(2) d (nm)
10.0	0.663	0.659	0.659*	0.659*
00.1	-------	0.291	r.a.	0.290
10.1	0.2668	0.266	0.266	0.264
20.1	0.2180	0.218	0.218	0.217
30.1	0.1753		0.174	0.176
00.2	0.1455	0.146	0.146	0.145
01.2	--------	0.142	0.143	0.141

Data for synthetic β-Si_3N_4 from Forgeng and Decker (1958). ------- = reflection not present. Data for meteoritic β-Si_3N_4 compiled from indexed $<11\bar{2}0>$ SAED patterns of β-Si_3N_4 whiskers in Inman (1) and Tieschitz (2). In these SAED patterns, no internal standard was available to calibrate the camera factor. The camera factor was calculated assuming a (10.0) spot spacing of 0.659 nm. These d-spacings (indicated by *), thus, by definition, agree perfectly with data from synthetic β-Si_3N_4. r.a. = reflection absent due to structure factors.

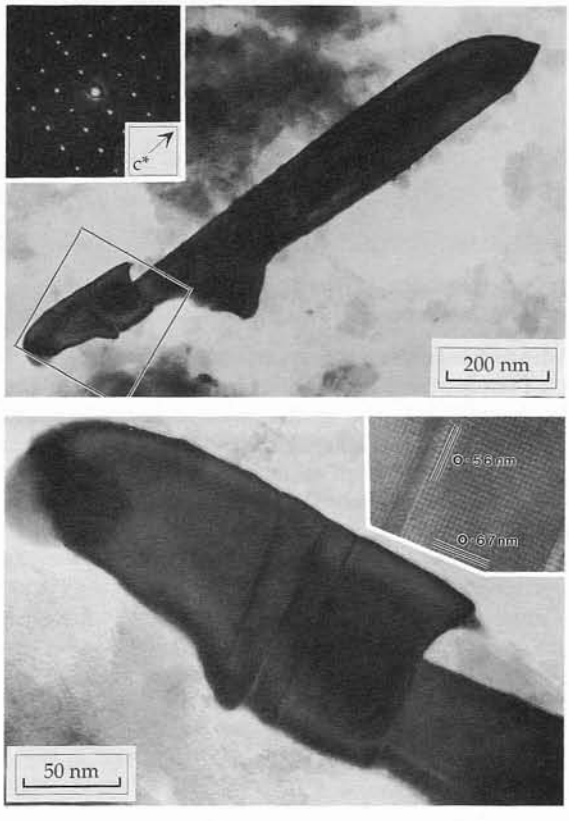

FIG. 5. A nierite crystal from Indarch that has a defect-rich nierite overgrowth. (a, upper) Bright-field TEM image and corresponding $<11\bar{2}0>$ SAED pattern of the crystal (inset). The lower left end of the crystal is overgrown by a defect-rich nierite crystal. The protuberance on the lower right-hand side of the main nierite lath may be another overgrowth but is more probably a contaminant from the residue, which is lying above or below the nierite crystal. (b, lower) Higher magnification image of the defect-rich nierite overgrowth (boxed area in 5a) and a corresponding high-resolution image (inset) of part of the overgrowth containing two planar defects.

Inman–In the Inman residue, nierite is considerably less abundant than in Indarch. Only one grain was found on every 120–180 μm^2 of C film examined. Two types of Si_3N_4 grains have been recognised. Most numerous are euhedral monomineralic laths (Fig. 6) and fibres of nierite, which are morphologically similar to those from Indarch. Their dimensions range from 630–3200 nm long (mean = 1830 nm) (n = 14) × 90–1700 nm wide (mean = 520 nm) with a length/width ratio of 1.3 to 19.3 (mean= 6.1). The laths are again oriented with their long axes parallel to c* (Fig. 6), and most are single crystals.

The other type of grain is represented by a single bimineralic object, 2.8 μm in length (Fig. 7). This grain comprises a typical euhedral lath of nierite, from the base of which projects a whisker (Fig. 7a), at whose tip is a crystallite of nierite (Fig. 7b). Interplanar angles and d-spacings from indexed SAED patterns from the whisker are comparable with those of synthetic β-Si_3N_4 (Table 6, column 1). High-resolution images again demonstrate that nierite crystals have an epitaxial relationship with the β-Si_3N_4 whisker, whereby $<11\bar{2}0>_{nierite} || <11\bar{2}0>_{\beta\text{-}Si_3N_4}$ (Fig. 7b). The long axis of this β-Si_3N_4 whisker is however elongate parallel to c* and so morphologically different to the β-Si_3N_4 bands in Indarch bimineralic grains whose long axes are normal to c* (*cf.*, Figs. 4 and 7).

A few SiC grains of unknown polytype, which range in size from 0.5 to 1.5 μm, were located in the Inman residue.

Tieschitz–Apparently, Si_3N_4 is rare in this residue; only two grains were found on > ~3000 μm^2 of C film examined. One grain was a tiny monomineralic lath of nierite, 440 nm long × 30 nm wide (length/width = 14.7). The other grain was a bimineralic whisker, 1600 nm long × 70 nm wide (length/width = 22.9) (Fig. 8a). The body of the whisker was sufficiently large for good SAED patterns to be obtained from a number of zone axes (Figs. 1d, 8a), and the calculated d-spacings and interplanar angles are consistent with β-Si_3N_4 (Table 6, column 2). The two tips of the whisker, which are of identical size and shape to each other, are nierite. The interface between nierite and β-Si_3N_4 is again sharp and oriented parallel to $(0001)_{\beta\text{-}Si_3N_4}$ (Fig. 8b). In common with the bimineralic grains from Indarch and Inman, there is an epitaxial relationship between nierite and β-Si_3N_4 whereby $<11\bar{2}0>_{nierite} || <11\bar{2}0>_{\beta\text{-}Si_3N_4}$ (Fig. 8a). This bimineralic whisker is crystallographically comparable to the composite grain from Inman, although the nierite crystals at either end of the β-Si_3N_4 whisker in Tieschitz are morphologically different to those of the Inman grain (*cf.*, Figs. 7 and 8).

Despite exhaustive study, only one crystal of SiC, 720 nm, was found in this residue.

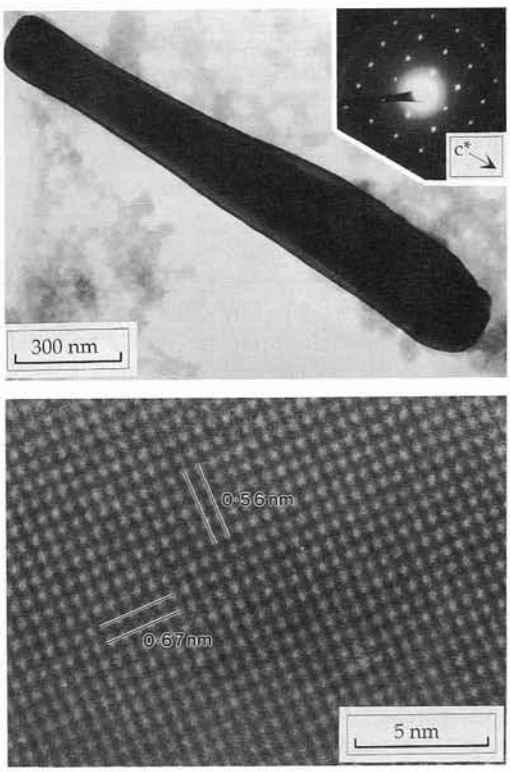

FIG. 6. Nierite from the Inman residue. (a, upper) Bright-field TEM image and corresponding $<11\bar{2}0>$ SAED pattern (inset) of a typical nierite crystal. (b, lower) High-resolution TEM image from part of a nierite crystal.

DISCUSSION

Previous Descriptions of Silicon Nitride in Meteorites

Previously, Si_3N_4 has been tentatively identified from acid-resistant residues of Indarch by Stone *et al.* (1991a,b) and Alexander *et al.* (1994) and from a residue of Tieschitz by Alexander (1993). The grains from Indarch described by Stone *et*

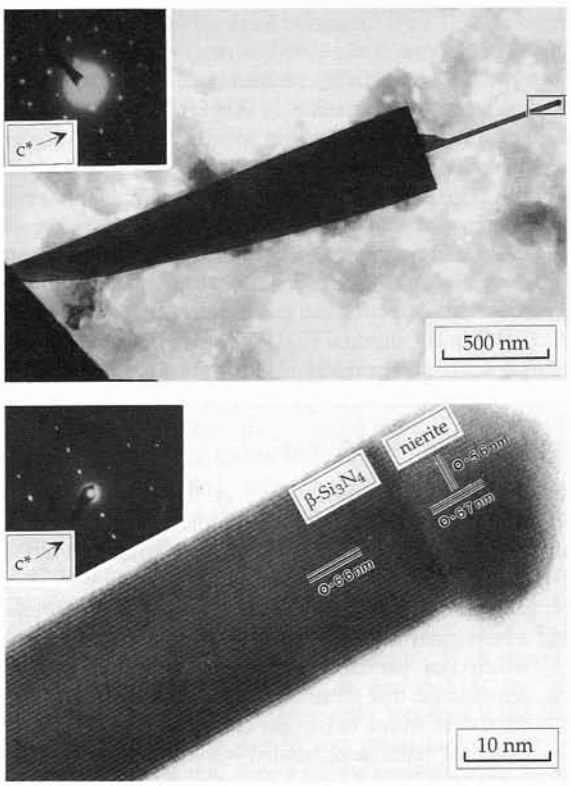

FIG. 7. The bimineralic Si_3N_4 grain from the Inman residue. (a, upper) Bright-field TEM image and corresponding $<11\bar{2}0>$ SAED pattern (inset) of the bimineralic grain. Most of the grain comprises a large nierite lath. However, projecting from the base of the lath (right hand side) is a whisker of β-Si_3N_4. At the very tip of the β-Si_3N_4 whisker is a crystallite of nierite. The SAED pattern indexes as nierite, but faint extra reflections from β-Si_3N_4 can be seen adjacent to some of the lower order nierite reflections. The feature in the lower left corner of the image is part of the Cu grid. (b, lower) High-resolution TEM image of the tip of the β-Si_3N_4 whisker (boxed area in 7a) and corresponding $<11\bar{2}0>$ SAED pattern of β-Si_3N_4 (inset). Note, in this SAED pattern, the (0001) and $(000\bar{1})$ reflections are absent.

al. (1991a,b) had smooth surfaces and were up to 20 μm. All of these previous identifications of meteoritic Si_3N_4 have been solely on the basis of chemical composition (using electron/ion microprobe) and so their crystallographic identity could not be determined.

Alexander *et al.* (1991, 1994) have also described Si_3N_4 from an acid-resistant residue of Qingzhen (EH3). They examined 58 grains of Si_3N_4, which ranged in size from 0.1 to 10.0 μm. Nine grains of Si_3N_4, 0.3–2.5 μm, were also found *in situ* within crystals of kamacite (α-Fe,Ni), perryite (Ni_xSi_y) and schreibersite (Fe_3P) from Qingzhen by Alexander *et al.* (1991, 1994), which they interpreted to have formed by exsolution from these minerals during parent-body metamorphism. This is supported by isotopic analyses, which indicate that Si_3N_4 in Qingzhen formed within the Solar System (Alexander *et al.*, 1991, 1994).

Sinoite (Si_2N_2O) occurs in some high petrologic grade enstatite chondrites including Hvittis (E6), Jajh deh Kot Lalu (E6), Pillistfer (E6), Ufana (E6) and Yilmia (E5) (Andersen *et al.*, 1964; Keil and Andersen, 1965a,b; Hoppe *et al.*, 1989). Sinoite was originally described by Andersen *et al.* (1964) from Jajh deh Kot Lalu, the meteorite in which it occurs as lath-like crystals up to 200 μm long in direct association with enstatite and with Fe,Ni metal. Thus, it is possible that in common with Si_3N_4 in Qingzhen, sinoite in some enstatite chondrites has also formed by exsolution during metamorphism. This is supported by the N-isotopic composition of Yilmia sinoite (Hoppe *et al.*, 1989), which is comparable to that of Qingzhen Si_3N_4. Importantly, we found one crystal of sinoite in a perchloric acid-resistant residue of Abee (EH4), but Si_3N_4 was absent. No sinoite was detected in any of the four Si_3N_4-bearing residues examined during this study, and Keil and Andersen (1965a) also failed to find sinoite in Indarch. These observations are in accordance with Alexander *et al.* (1994) who suggest that Si_3N_4 and sinoite are mutually exclusive in their occurrence in enstatite chondrites. Kinetic factors may have inhibited the formation of sinoite in low petrologic grade enstatite chondrites such as Indarch (EH4) and Qingzhen (EH3), but these factors were overcome during higher temperature metamorphism (~900–1100 °C) of the E5 and E6 meteorites (Alexander *et al.*, 1994).

Structure and Growth of Nierite

The majority of nierite crystals in Indarch and Inman are interpreted to have grown as μm-sized laths or fibres. Few nierite crystals were imaged in cross-section (*i.e.*, parallel to <0001>) during this study, but Alexander *et al.* (1994, their Fig. 3) observed a Si_3N_4 grain (polymorph unknown) within Qingzhen schreibersite that had a hexagonal shape, probably a (0001) section. Thickness fringes, which run parallel to the margins of nierite laths in Indarch, demonstrate that these crystals thin towards their margins, which is consistent with a hexagonal cross-sectional morphology.

The euhedral habit and limited variation in size of nierite crystals from Indarch and Inman indicates that their growth was unrestricted and that physico-chemical conditions during crystallization were relatively invariant. Additionally, the scarcity of intergrown nierite crystals suggests that most formed at least 5 μm apart. Some nierite laths in Indarch have been epitaxially overgrown by small, defect-rich nierite crystals (Fig. 5). The gap in time between the main episode of nierite crystallization and formation of the defect-rich overgrowth is not known. This second phase of nierite crystallization was however probably of a much shorter duration than the first and main episode.

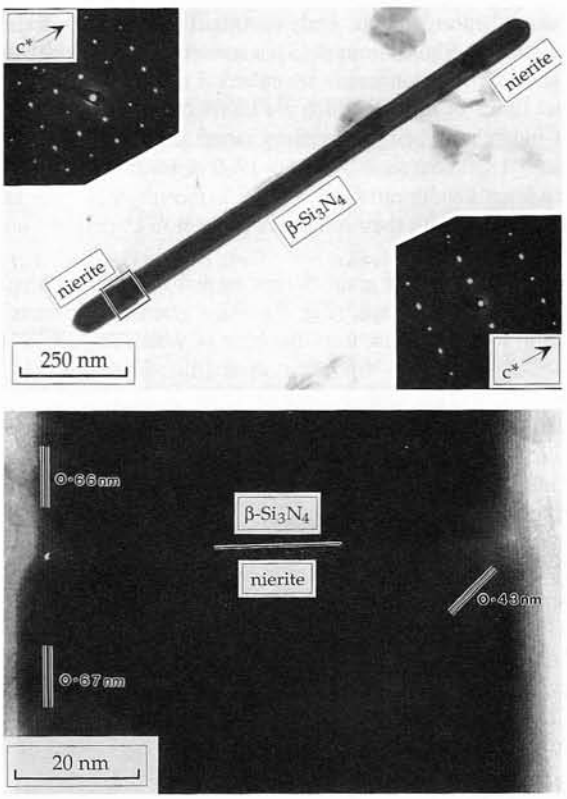

FIG. 8. The bimineralic Si_3N_4 grain from the Tieschitz residue. (a, upper) Bright-field TEM image and corresponding $<11\bar{2}0>$ SAED patterns (inset) of the whisker. The main body of the whisker is β-Si_3N_4 (lower right SAED pattern), whereas, the two tips, which are of identical size and shape, are nierite (upper left SAED pattern). (b, lower) High resolution TEM image of the interface between nierite and β-Si_3N_4 (boxed area in 8a). Note that the interface between β-Si_3N_4 and nierite is planar and parallel to (0001). Because the whisker increases in thickness towards its centre, lattice fringes are most easily visible at the margins of the grain.

Origin of Nierite

Niihara and Hirai (1979) have documented synthetic α-Si_3N_4 needles, which have been grown experimentally by chemical vapour deposition. These synthesised needles have a hexagonal cross-section and grew most rapidly along their c-axes and so are morphologically comparable to nierite crystals from Indarch and Inman. Thus, nierite crystals from these meteorites may have grown by chemical vapour deposition in solar nebula or circumstellar gas prior to incorporation in to the part of the parent body from which the meteorite was later derived. However, the occurrence of Si_3N_4 grains only in kamacite, perryite and schreibersite from Qingzhen (Alexander *et al.*, 1994) argues against a preaccretionary origin for Si_3N_4 in enstatite chondrites at least, and is consistent with formation by parent-body metamorphism.

In order to test the possibility that Si_3N_4 in the Indarch residue could also have formed by exsolution, some metal, phosphide and sulphide grains in a thin section of Indarch were analysed by electron microprobe. No Si_3N_4 was found *in situ* during these analyses, but we cannot deny its existence at low abundance because we did not use the automatic mapping technique of Swan *et al.* (1989) and Alexander *et al.* (1994), which has been very successful in finding such grains.

Electron microprobe analyses of kamacite, schreibersite and troilite in Indarch and the same minerals plus perryite in Qingzhen are presented in Table 7. Kamacite in Indarch has significant concentrations of elemental Si in solid solution (average of 2.8 wt%; n = 12), indeed comparable to that seen in Qingzhen (average of 2.5 wt%; n = 12) from which Si_3N_4 has exsolved (Alexander *et al.*, 1991, 1994). Schreibersite in Indarch and Qingzhen has lower concentrations of Si (<0.5 wt% in both meteorites), although it did exsolve Si_3N_4 in Qingzhen. Troilite in both meteorites contains <0.1 wt% Si and so is unlikely to have been a source of Si. Other measurements of Si concentrations in Indarch kamacite are comparable (3.3–3.6 wt%, Keil, 1968; 2.7–3.2 wt%, Wasson and Wai, 1970; 3.11 wt% mean, Leitch and Smith, 1982). The concentrations of Si in Indarch schreibersite given here are also similar to values recorded by Keil (1968) (0.16–0.24 wt%) and Leitch and Smith (1982) (0.2 wt% average). No perryite was found in the thin section of Indarch during this study, but it has been recorded from Indarch by Ramdohr (1963).

Muenow *et al.* (1992) reported 110–430 ppm N released from enstatite chondrites due to melting of the Fe,Ni-sulphide cotectic. They concluded that the N possibly occurs within sulphides. Hashizume and Sugiura (1992) showed that the metal of equilibrated H-type chondrites (H4–H6) contains 1.17 to >2 ppm N. This N is found in the metal, and its concentration increases with metamorphic grade of the host meteorite. It is possible that unequilibrated H-type ordinary chondrites such as Tieschtiz also contain N-bearing metal. Iron meteorites can also have significant concentrations of N. Recorded values range from 0.5 to 224 ppm (Shukla and Goel, 1981) and ~0.2 to 80 ppm (Franchi *et al.*, 1993). The majority of the N in iron meteorites is suggested by Franchi *et al.* (1993) to be dissolved in Fe,Ni metal, both kamacite (α-Fe,Ni) and taenite (γ-Fe,Ni).

One area of Indarch point counted by Keil (1968) contained 17.5 wt% metallic Fe,Ni, 7.3 wt% troilite and 1.1 wt% schreibersite. Thus, with regard to Indarch at least, sufficient Si and N was probably available from these minerals to exsolve the quantity of nierite recorded during parent-body metamorphism. No data could be found regarding metal abundances in Inman, but Hutchison *et al.* (1981) recorded 15.21 wt% kamacite and 0.62 wt% taenite in Tieschitz (total of 15.63 wt% metallic Fe,Ni). No published analyses of Si concentrations in Tieschitz kamacite were found. However, Si concentrations of <0.3–4.5 mg/g have been reported from Fe,Ni metal (kamacite/tetrataenite/taenite) of the ordinary chondrites Bishunpur (LL3.1), Chainpur (LL3.4) and Krymka (LL3.1) by Rambaldi *et al.* (1980) and Rambaldi and Wasson (1981, 1984). Recently, Zanda *et al.* (1994) have shown that in most cases the Si in ordinary chondrite metal is not present in solid solution but as small inclusions that formed by exsolution during cooling of their host chondrules or accompanying metamorphism. Silicon in solid solution only occurs in metal from the least metamorphosed chondrites studied by them, namely Murchison (CM2) and Semarkona (LL3.0). These observations by Zanda *et al.* (1994) suggest that it is a reasonable hypothesis that Si-rich minerals such as Si_3N_4 may have formed by exsolution from metal during metamorphism of ordinary chondrites.

TABLE 7. Representative electron microprobe analyses of Si_3N_4-bearing and potentially Si_3N_4-bearing minerals in Qingzhen and Indarch.

	Schreibersite		Kamacite		Troilite		Perryite
	Q	I	Q	I	Q	I*	Q
Si	0.2	0.2	2.4	2.7	0.1	n.d.	11.6
P	14.4	15.1	n.d.	0.1	n.d.	n.d.	3.4
S	n.d.	0.1	0.1	0.1	37.3	37.0	n.d.
Cr	n.d.	n.d.	n.d.	n.d.	1.3	1.4	0.1
Fe	70.7	67.6	94.4	89.9	61.2	60.5	8.4
Ni	13.5	17.1	3.0	6.5	0.1	n.d.	76.6
Sum:	98.8	100.1	99.9	99.3	100.0	98.9	100.1

Q = Qingzhen, **I** = Indarch.
*Leitch and Smith (1982) reported 0.26 wt% Ti (? TiN inclusion) and 1.01 wt% Mn from Indarch troilite.

Formation of β-Silicon Nitride

The β-Si_3N_4 crystals in Indarch, Inman and Tieschitz could have formed by recrystallization of nierite (or *vice versa*) or one polymorph of Si_3N_4 may have predated the other and acted as a seed for its later growth. Bimineralic grains of α- and β-Si_3N_4 are commonplace in synthetic Si_3N_4 ceramics (*i.e.*, Ning *et al.*, 1992). Despite the industrial importance of these materials, the determinants of whether α- and β-Si_3N_4 forms during manufacture are still poorly understood (Ziegler *et al.*, 1987). Synthetic α-Si_3N_4 is generally considered to be the more energy-rich polymorph, which becomes unstable with respect to β-Si_3N_4, and transforms into it by solution-precipitation at temperatures of >1650 °C (*i.e.*, α- and β-Si_3N_4 are low- and high-temperature polymorphs, respectively) (Drew and Lewis, 1974; Grun, 1979; Lange *et al.*, 1991). The converse β to α transition, producing α-Si_3N_4 polymorphs of β-Si_3N_4 crystals, has been reported by Clancy (1974) but is very rare (Ziegler *et al.*, 1987). The sharp, crystallographically-controlled interface between nierite and β-Si_3N_4 in meteorite residues, the significant difference in habit between the nierite laths and β-Si_3N_4 whiskers and the very high temperatures required for the synthetic α to β transformation, argues against formation of β-Si_3N_4 by recrystallization of nierite. The same constraints mean that it is highly unlikely that nierite in the bimineralic grains has formed by partial transformation of β-Si_3N_4 precursor.

The other possibility is that β-Si_3N_4 crystals predated nierite and acted as seeds from which some nierite crystals later grew. This is supported by the limited petrographic evidence. Bimineralic laths in Indarch are normally symmetrical either side of the medial β-Si_3N_4 band when viewed down $<11\bar{2}0>$ (Fig. 4a). This is interpreted to indicate that the two nierite crystals grew outwards, parallel to c*, from the exposed (0001) surfaces of the preexisting β-Si_3N_4 band. The same appears true for the Tieschitz bimineralic whisker. However, in the case of this grain, there may have been only limited growth of nierite such that euhedral laths were unable to form. With regard to the Inman bimineralic grain, at one end of the β-Si_3N_4 whisker a nierite lath grew fully, whereas at the other end for some reason growth was much more limited. This may suggest that during nierite crystallization, one end of the β-Si_3N_4 whisker was in partial contact with another phase, or that one (0001) face of β-Si_3N_4 became chemically contaminated such that nierite could not grow beyond a crystallite.

The gap in time between the growth of the β-Si_3N_4 whiskers and crystallization of nierite overgrowths cannot be determined. What is clear is that following formation of β-Si_3N_4 whiskers, the physico-chemical environment around them changed such that nierite was stable and

crystallized on the β-Si_3N_4 substrate. Importantly, no β-Si_3N_4 crystals were found without nierite overgrowths. This could be because the β-Si_3N_4 whiskers are very small and so difficult to locate by TEM when not attached to a larger nierite crystal. However, it could also indicate that nierite and β-Si_3N_4 formed in the same environment, which rapidly switched from β-Si_3N_4 to nierite crystallization so that all previously formed β-Si_3N_4 crystals acquired nierite overgrowths. The scarcity of β-Si_3N_4 crystals relative to nierite in Indarch and Inman however indicates that nierite laths could just as easily grow without as with a β-Si_3N_4 whisker seed.

Contrasts in the Abundance of Nierite and β-Silicon Nitride

Qualitatively, the abundance of nierite in the three meteorite residues decreases from Indarch to Inman to Tieschitz, but β-Si_3N_4 is equally rare in all three. Thus, although it is a very minor phase in Indarch and Inman, β-Si_3N_4 is volumetrically more abundant than nierite in Tieschitz. The reasons for these differences in abundance are interpreted to be a combination of formation and destruction factors. The primary control on the initial abundance of nierite is interpreted to have been the quantity of kamacite, perryite and schreibersite present and the concentration of Si and N in these minerals. Although Indarch and Tieschitz contain a similar quantity of Fe,Ni metal (17.5 and 15.63 wt% respectively), the initial concentration of Si and N in the metal of ordinary chondrites was probably much lower. The reason why β-Si_3N_4 comprises a much higher proportion of total Si_3N_4 in Tieschitz than Inman is probably a metamorphic effect with the nierite, which is less stable at higher temperatures than β-Si_3N_4, being preferentially destroyed. Thus, the nierite/β-Si_3N_4 ratio is lower in the meteorite of the higher metamorphic grade (Tieschitz). In addition, oxidation during metamorphism may have played an important role in the destruction of nierite.

Suggestions for Further Work

An essential next step in the study of nierite and β-Si_3N_4 is to find these minerals *in situ* within meteorite samples, both in enstatite chondrites such as Indarch and, more importantly, the ordinary chondrites including Inman and Tieschitz. This will help in understanding how and when these minerals were formed. However, Si_3N_4 is very scarce in the bulk meteorites (706, 148, 27 and 12 ppb in Indarch, Adrar 003, Inman and Tieschitz, respectively; Russell *et al.*, 1995). So even using the automatic mapping technique of Swan *et al.* (1989) and Alexander *et al.* (1994), these grains would be very difficult to locate and analyse *in situ*. This is especially true for the tiny β-Si_3N_4 whiskers (the Tieschitz bimineralic whisker, viewed normal to (0001), would have a surface area of ~0.01 μm^2).

We have described the first natural occurrence of the hexagonal polymorph of Si_3N_4 (β-Si_3N_4) but discovered too few crystals for an unambiguous determination of its chemical composition and crystallographic properties. However, with a sufficient quantity of acid-resistant residue of Inman, Tieschitz or another ordinary chondrite, it should be possible to obtain enough data for this compound to be recognised as a new mineral and named. If enough acid-resistant residue of an enstatite chondrite such as Indarch or Qingzhen were available, a more accurate determination of the unit-cell parameters of nierite, by x-ray diffraction, should also be possible.

No TEM studies of acid-resistant residues of low petrologic type ordinary chondrites have been undertaken. The possibility that nitrides existed in the samples studied here was only realised because interstellar SiC was of low abundance and, hence, did not mask the existence of high-stability nitrides in stepped combustion data (Russell *et al.*, 1995). Thus, it may be most profitable to search for Si_3N_4 in the least metamorphosed unequilibrated ordinary chondrites. By studying a sequence of unequilibrated ordinary chondrites of the same chemical class but different metamorphic grades, it may be easier to evaluate the roles of metamorphism and oxidation in the destruction of nierite.

SUMMARY

Two crystallographically and petrographically distinct Si nitrides have been identified in perchloric acid-resistant residues of the meteorites Indarch, Inman and Tieschitz. The most abundant nitride, which is crystallographically and chemically equivalent to synthetic α-Si_3N_4, has been approved by the International Mineralogical Association as a new mineral and named nierite. The other nitride is extremely rare, and only two crystals were found that were sufficiently large to provide single-crystal SAED patterns. This phase is inferred to be equivalent to β-Si_3N_4, which is the hexagonal polymorph of synthetic Si_3N_4.

Euhedral single crystals of nierite in Indarch are interpreted to have formed by exsolution of Si and N from kamacite, perryite and schreibersite during parent body metamorphism. A few nierite laths in Indarch are epitaxially overgrown by smaller defect-rich nierite crystals, indicating that in some contexts there were two discrete episodes of nierite crystallization. The origin of nierite in Adrar 003, Inman and Tieschitz cannot be determined by study of the meteorite residues alone. These minerals need to be located *in situ* within intact meteorite samples. Whiskers of β-Si_3N_4, which occur in the Indarch, Inman and Tieschitz residues are, in all cases, epitaxially overgrown by nierite crystals. Although the β-Si_3N_4 whiskers predate their nierite overgrowths, the timing and environment of β-Si_3N_4 crystallization is not known.

By analogy with studies of Si_3N_4 found *in situ* within samples of Qingzhen, the much greater abundance of Si_3N_4 in the enstatite chondrite Indarch than in the two ordinary chondrites Inman and Tieschitz is probably due to differences in the volume of Si- and N-bearing kamacite, perryite and schreibersite between the two classes of meteorites. Additionally, Inman may have a greater abundance of nierite and a higher nierite/β-Si_3N_4 ratio than Tieschitz because of the relatively greater degree of destruction of nierite in Tieschitz during metamorphism, possibly accompanied by oxidation. Stable isotopic results from these residues (Russell *et al.*, 1995) suggest that those grains that were most resistant to destruction within the parent body (mainly β-Si_3N_4) are enriched in ^{15}N and possibly presolar in origin.

Acknowledgements–We would like to thank Keith Moulding and Brian Diamond (University of Essex) for the assistance with the TEM and David Barber (D.B.) for his help throughout this research project. Quantitative chemical analyses of nierite grains were performed by Robert Keyse (University of Liverpool) using a STEM run jointly by the Materials Science departments of the Universities of Manchester and Liverpool and is supported by a grant from SERC. David Hulmes provided access to the CM12 TEM in the Department of Biochemistry, University of Edinburgh. Electron microprobe analyses were performed with the assistance of Stuart Kearns (University of Edinburgh). We are grateful to the British Museum (Natural History) for the loan of a thin section of Indarch, Conel Alexander for a sample of Qingzhen and Ed Olsen, Robert Hutchison, G. Kurat and Elbert King for samples used to make the residues. Help with finding published data on synthetic Si_3N_4 was kindly given by Frank Riley (University of Leeds) and W. Kurtz and F. A. Schroder (Gmelin-Institut, Frankfurt). Joe Mandarino, Klaus Keil and Ian Parsons gave considerable help with the new mineral proposal. This paper benefitted considerably from reviews by Conel Alexander and Klaus Keil. This

research was funded by grants from NERC (to D.B.) and SERC, now PPARC, (to C.T.P).

Editorial handling: K. Keil

REFERENCES

ALEXANDER C. M. O'D. (1993) Presolar SiC in chondrites: How variable and how many sources? *Geochim. Cosmochim. Acta* **57,** 2869–2888.

ALEXANDER C. M. O'D., PROMBO C. A., SWAN P. D. AND WALKER R. M. (1991) SiC and Si_3N_4 in Qingzhen (EH3) (abstract). *Lunar Planet. Sci.* **22,** 5–6.

ALEXANDER C. M. O'D., SWAN P. AND PROMBO C. A. (1994) Occurrence and implications of silicon nitride in enstatite chondrites. *Meteoritics* **29,** 79–85.

AMARI S., ANDERS E., VIRAG A. AND ZINNER E. (1990) Interstellar graphite in meteorites. *Nature* **345,** 238–240.

ANDERSEN C. A., KEIL K. AND MASON B. (1964) Silicon oxynitride: A meteoritic mineral. *Science* **146,** 256–257.

BANNISTER F. A. (1941) Osbornite, meteoritic titanium nitride. *Min. Mag.* **26,** 36–44

BERNATOWICZ T., FRAUNDORF G., MING T., ANDERS E., WOPENKA B., ZINNER E. AND FRAUNDORF P. (1987) Evidence for interstellar SiC in the Murray carbonaceous meteorite. *Nature* **330,** 728–730.

BERNATOWICZ T., AMARI S., ZINNER E. K. AND LEWIS R. S. (1991) Interstellar grains within interstellar grains. *Astrophys. J.* **373,** L73–L76.

CLANCY W. P. (1974) A limited crystallographic and optical characterisation of alpha and beta silicon nitride. *Microscope* **22,** 279–315.

CLIFF G. AND LORIMER G. (1975) The quantitative analysis of thin specimens. *J. Microscopy* **103,** 203–207.

DREW P. AND LEWIS M. H. (1974) The microstructures of silicon nitride ceramics during hot-pressing transformations. *J. Mat. Sci.* **9,** 261–269.

FORGENG W. D. AND DECKER B. F. (1958) Nitrides of silicon. *Trans. Metal. Soc. AIME* **212,** 343–348.

FRANCHI I. A., WRIGHT I. P. AND PILLINGER C. T. (1993) Constraints on the formation conditions of iron meteorites based on N concentrations and isotopic measurements. *Geochim. Cosmochim. Acta* **57,** 3105–3121.

GRADY M. M., WRIGHT I. P., CARR L. P. AND PILLINGER C. T. (1986) Compositional differences in enstatite chondrites based on carbon and nitrogen stable isotope measurements. *Geochim. Cosmochim. Acta* **50,** 2799–2813.

GRUN R. (1979) The crystal structure of β-Si_3N_4: Structural and stability considerations between α- and β-Si_3N_4. *Acta. Cryst.* **B35,** 800–804.

HARDIE D. AND JACK K. H. (1957) Crystal structure of silicon nitride. *Nature* **180,** 332–333.

HASHIZUME K. AND SUGIURA N. (1992) Various nitrogen compositions in H-chondrite metal (abstract). *Meteoritics* **27,** 232.

HOPPE P., GEISS J. AND EL GORESY A. (1989) Nitrogen isotopes in sinoite grains of the Yilmia enstatite chondrite (abstract). *Meteoritics* **24,** 278.

HOPPE P., STREBEL R. AND EBERHARDT P. (1994) Evidence for an interstellar nitride grain with highly anomalous isotopic compositions of C, N and Si (abstract). *Lunar Planet. Sci.* **25,** 563–564.

HUSS G. R., HUTCHEON I. D., WASSERBURG G. J. AND STONE J. (1992) Presolar (?) corundum in the Orgueil meteorite (abstract). *Lunar Planet. Sci.* **23,** 563–564.

HUSS G. R., FAHEY A. J. AND WASSERBURG G. J. (1995) Si and C isotopes in SiC from the Qingzhen (EH3) chondrite (abstract). *Lunar Planet. Sci.* **26.** 645–646.

HUTCHISON R., BEVAN A., EASTON A. J. AND AGRELL S. O. (1981) Mineral chemistry and genetic relations among H-group chondrites. *Proc. Royal Soc. London A* **374,** 159–178.

JACK K. H. (1983) The characterisation of α'-sialons and the α-β relationships in sialons and silicon nitrides. In *Progress in Nitrogen Ceramics* (ed. F. L. Riley), pp. 45–60. Martinus Nijhoff, The Netherlands.

KATO K., INOUE Z., KIJIMA K., KAWADA I., TANAKA H. AND YAMANE T. (1975) Structural approach to the problem of oxygen content in alpha silicon nitride. *J. Amer. Ceram. Soc.* **58,** 90–91.

KEIL K. (1968) Mineralogical and chemical relationships among enstatite chondrites. *J. Geophys. Res.* **73,** 6945–6976.

KEIL K. AND ANDERSEN C. A. (1965a) Occurrences of sinoite, Si_2N_2O, in meteorites. *Nature* **207,** 745.

KEIL K. AND ANDERSEN C. A. (1965b) Electron microprobe study of the Jajh deh Kot Lalu enstatite chondrite. *Geochim. Cosmochim. Acta* **29,** 621–632.

KOHATSU I. AND MCCAULEY J. W. (1974) Re-examination of the crystal structure of α-Si_3N_4. *Mat. Res. Bull.* **9,** 917–920.

LANGE H., WÖTTING G. AND WINTER G. (1991) Silicon nitride-from powder synthesis to ceramic materials. *Angew. Chem. Int. Ed. Engl.* **30,** 1579–1597.

LEE M. R., RUSSELL S. S., ARDEN J. W. AND PILLINGER C. T. (1992) The isotopic composition and mineralogy of silicon nitride (Si_3N_4) within ordinary and enstatite chondrites (abstract). *Meteoritics* **27,** 248–249.

LEITCH C. A. AND SMITH J. V. (1982) Petrography, mineral chemistry and origin of Type I enstatite chondrites. *Geochim. Cosmochim. Acta* **46,** 2083–2097.

LEWIS R. S., MING T., WACKER J. F., ANDERS E. AND STEEL E. (1987) Interstellar diamonds in meteorites. *Nature* **326,** 160–162.

LEWIS R. S., ANDERS E. AND DRAINE B. T. (1989) Properties, delectability and origin of interstellar diamonds in meteorites. *Nature* **339,** 119–121.

MARCHAND P. R., LAURENT Y. AND LANG J. (1969) Structure du niture de silicum. *Acta Cryst.* **B25,** 2157–2160.

MUENOW D. W., KEIL K. AND WILSON L. (1992) High temperature mass spectrometric degassing of enstatite chondrites: Implications for pyroclastic volcanism on the aubrite parent body. *Geochim. Cosmochim. Acta* **56,** 4267–4280.

NIER A. O. (1950) A redetermination of the relative abundances of the isotopes of carbon, nitrogen, oxygen, argon and potassium. *Phys. Review* **77,** 789–793.

NIIHARA K AND HIRAI T. (1979) Growth morphology and slip system of a α-Si_3N_4 single crystal. *J. Mat. Sci.* **14,** 1952–1960.

NING X. G., PAN J., HU K. Y., YE H. Q. AND FUKUNAGA H. (1992) Transmission electron microscopy studies on the microstructure of a β-Si_3N_4/6061Al composite. *J. Mat. Sci. Lett.* **11,** 558-561.

NITTLER L. R., WALKER R. M. AND ZINNER E. (1993) Identification of an interstellar oxide grain from the Murchison meteorite by ion imaging (abstract). *Lunar Planet. Sci.* **24,** 1087–1088.

PRIEST H. F., BURNS F. C., PRIEST G. L. AND SKAAR E. C. (1973) Oxygen content of alpha silicon nitride. *J. Am. Ceram. Soc.* **56,** 395.

RAMBALDI E. R. AND WASSON J. T. (1981) Metal and associated phases in Bishinpur, a highly unequilibrated ordinary chondrite. *Geochim. Cosmochim. Acta* **45,** 1001–1015.

RAMBALDI E. R. AND WASSON J. T. (1984) Metal and associated phases in Krymka and Chainpur: Nebular formational processes. *Geochim. Cosmochim. Acta* **48,** 1885–1897.

RAMBALDI E. R., SEARS D. W. AND WASSON J. T. (1980) Si-rich Fe-Ni grains in highly unequilibrated chondrites. *Nature* **287,** 817–820.

RAMDOHR P. (1963) The opaque minerals in stony meteorites. *J. Geophys. Res.* **68,** 2011–2063.

RUDDLESDEN S. N. AND POPPER P. (1958) On the crystal structures of the nitrides of silicon and germanium. *Acta Cryst.* **11,** 465–468.

RUSSELL S. S., ARDEN J. W. AND PILLINGER C. T. (1991). Evidence for multiple sources of diamond from primitive chondrites. *Science* **254,** 1188–1191.

RUSSELL S. S., ARDEN J. W. AND PILLINGER C. T. (1992a) The effects of metamorphism on chondritic diamond and silicon carbide (abstract). *Meteoritics* **27,** 283.

RUSSELL S. S., PILLINGER C. T. ARDEN J. W., LEE M. R. AND OTT U. (1992b) A new type of meteoritic diamond in the enstatite chondrite Abee. *Science* **256,** 206–209.

RUSSELL S. S., LEE M. R., ARDEN J. W. AND PILLINGER C. T. (1995) The isotopic composition and origins of silicon nitride in the ordinary and enstatite chondrites. *Meteoritics* **30,** 399–404.

SASAKI K., KURODA K., IMURA T., SAKA H. AND KAMINO T. (1985) Determination of the displacement vector of planar defects in α-silicon nitride whisker by means of high resolution electron microscopy. *J. Electron. Microsc.* **34,** 414–418.

SHUKLA P. N. AND GOEL P. S. (1981) Total nitrogen in iron meteorites. *Earth Planet. Sci. Lett.* **52,** 251–258.

STONE J., HUTCHEON I. D., EPSTEIN S. AND WASSERBURG G. J. (1991a) Correlated Si isotope anomalies and large ^{13}C enrichments in a family of exotic SiC grains. *Earth Planet. Sci. Lett.* **107,** 570–581.

STONE J., HUTCHEON I. D., EPSTEIN S. AND WASSERBURG G. J. (1991b) Silicon, carbon and nitrogen isotopic studies of silicon carbide in carbonaceous and enstatite chondrites. In *Stable Isotope Geochemistry: A tribute to Samuel Epstein* (eds. H. P. Taylor, J. R. O'Neil and I. R. Kaplan), pp. 487–504. The Geochemical Society, Special Publication 3.

SWAN P. S., WALKER R. M. AND YUAN J. (1989) Location of small SiC crystals in meteorites using a low-voltage X-ray mapping technique (abstract). *Lunar Planet. Sci.* **20,** 1093–1094.

TAYLOR D. (1973) Reflected light microscopy of silicon nitride and oxynitride. *Trans. J. Brit. Ceram. Soc.* **72,** 319–321.

VERCHOVSKY A. B., FRANCHI I. A., ARDEN J. W., FISENKO A. V., SEMIONOVA L. F. AND PILLINGER C. T. (1993) Cojoint release of N, C, He and Ar from

C_δ by stepped pyrolysis: Implications for the identification of their carriers (abstract). *Meteoritics* **28,** 452–453.

WASSON J. T. AND WAI C. M. (1970) Composition of the metal, schreibersite and perryite of enstatite achondrites and the origin of enstatite chondrites and achondrites. *Geochim. Cosmochim. Acta* **34,** 169–184.

WILD S., GRIEVESON P. AND JACK K. H. (1972) The crystal structures of alpha and beta silicon and germanium nitrides. In *Special Ceramics* 5 (ed. P. Popper), pp. 385–393. British Ceramic Research Association, Stoke-on-Trent.

WRIGHT I. P. (1992) Stardust memories. *Nature* **356,** 567–568.

ZANDA B., BOUROT-DENISE M., PERRON C. AND HEWINS R. H. (1994) Origin and metamorphic redistribution of silicon, chromium, and phosphorous in the metal of chondrites. *Science* **265,** 1846–1849.

ZIEGLER G., HEINRICH J. AND WOTTING G. (1987) Relationships between processing, microstructure and properties of dense and reaction-bonded silicon nitride. *J. Mat. Sci.* **22,** 3041–3086.